

Properties of superconductivity on the density wave background with small ungapped Fermi surface pockets.

P. D. Grigoriev*

L. D. Landau Institute for Theoretical Physics, Chernogolovka, Russia[†]

(Dated: December 1, 2018)

We investigate the properties and the microscopic structure of superconductivity (SC), coexisting and sharing the common conducting band with density wave (DW). Such coexistence may take place when the nesting of the Fermi surface (FS) is not perfect, and in the DW state some quasi-particle states remain on the Fermi level and lead to the Cooper instability. The dispersion of such quasi-particle states is, in general, very different from that without DW. Therefore, the properties of SC on the DW background may strongly differ from those without DW. The upper critical field H_{c2} in such a SC state increases as the system approaches the critical pressure, where the ungapped quasi-particles and superconductivity just appear, and it may considerably exceed the usual H_{c2} value without DW. The SDW background strongly suppresses the singlet SC pairing, while it does not affect so much the triplet SC transition temperature. The results obtained explain the experimental observations in layered organic metals $(\text{TMTSF})_2\text{PF}_6$ and $\alpha\text{-(BEDT-TTF)}_2\text{KHg(SCN)}_4$, where SC appears in the DW states under pressure and shows many unusual properties.

PACS numbers: 71.30.+h, 74.70.Kn, 75.30.Fv

I. INTRODUCTION

The interplay between superconductivity (SC) and insulating charge or spin density wave states is a subject of an active investigation for more than 30 years (for a review see, e.g., Ref. [1]). The density wave (DW) is traditionally considered as a strong obstacle for the formation of SC, because it creates an energy gap on the Fermi level.^{2,3,4} The coexistence of DW and SC has been considered in metals with several conducting bands or with imperfect nesting, when even in the DW state there is a finite electron density on the Fermi level.^{5,6,7} Then the transition temperature T_c^{SC} to the SC state reduces exponentially when the DW is formed, because the electrons, participating in the formation of DW, drop out from the SC condensate.^{5,6}

However, in several compounds [e.g., in layered organic superconductors $(\text{TMTSF})_2\text{PF}_6$ and $\alpha\text{-(BEDT-TTF)}_2\text{KHg(SCN)}_4$],^{8,9} the SC transition temperature on the DW background is very close to (or even exceeds) T_c^{SC} without DW. In $(\text{TMTSF})_2\text{PF}_6$ superconductivity coexists with spin-density-wave (SDW) state at temperature below $T_c^{SC} \approx 1.1\text{K}$ in the pressure interval above some critical pressure $P_{c1} \approx 8.5\text{kbar}$, but below $P_c \approx 9.5\text{kbar}$, at which the SDW phase undergoes the 1st order phase transition into metallic state.⁸ This fact is even more surprising, because this compound has only one quasi-one-dimensional (Q1D) conducting band. A special attention was given to the fact, that the upper critical field H_{c2} in this superconducting state exceeds several times the expected paramagnetic limit,¹⁰ (see Refs. [11,12]), and no change in the Knight shift has been observed in this compound as temperature lowers to this SC state¹³. Both these features suggest the spin-triplet superconducting pairing in $(\text{TMTSF})_2\text{PF}_6$. In addition, the upper critical field H_{c2} perpendicular to the conducting layers strongly increases as pressure

approaches P_{c1} and has an unusual upward curvature as function of temperature¹⁴, suggesting that the SDW has a very strong influence on the SC properties of this phase. The electronic structure of this mixed phase is still under debates. A phase separation in a form of macroscopic metal and DW domains,^{8,14} being natural with the constant volume constraint, seems strange at fixed pressure, when the whole sample may choose the state with the lowest free energy. The pressure and temperature dependence of the upper critical field requires,¹⁴ that the size d of the SC domains, if they exist, must be much less than the SC coherence length $\xi_{SC} \sim 10^{-4}\text{cm}$ as pressure approaches P_{c1} [see Eq. (59) and the discussion in Sec. III]. This raises many questions about the structure of such a mixed state, because if the domain width is comparable to the SDW coherence length, this confinement of the electron wave functions costs additional energy greater than the SC energy gap. The angular magnetoresistance oscillations¹⁵ do not give a definite test whether the spatial phase separation occurs on a scale greater than the SC coherence length.

An alternative to the picture^{8,14} of macroscopic DW and normal (or SC) domains in $(\text{TMTSF})_2\text{PF}_6$ has been proposed recently.^{16,17} According to Ref.¹⁷, there are two different structures where SC coexists microscopically with DW. In the first structure, the destruction of the insulating DW phase at $P > P_{c1}$ goes via forming the ungapped metallic pockets in the electronic spectrum, that spread over the momentum space, merging into the normal metallic state gradually or via a phase transition. This scenario, looking similar to the one studied in Refs. [5,6], however, differs from it, because the formation of DW strongly modifies the quasi-particle dispersion in the ungapped parts of the Fermi surface, changing the properties of SC state on the DW background. In the second scenario, the DW order parameter at pressure $P > P_{c1}$ becomes spatially nonuniform by means of

amplitude solitons. These soliton structures are familiar in charge-density-wave (CDW) states at high pressure or in magnetic field (see, e.g., reviews in Refs. [18],[19]). The normal or SC phase appears first as the metallic domain walls, and the concentration of these soliton walls increases with increasing pressure. At finite density of solitons, i.e. above P_{c1} , the electron wave functions of single solitons strongly overlap, forming a new periodic conducting metallic network on the DW background. If it were not for the 1st order transition with the further increase of soliton density, the new phase is expected to merge gradually into the normal state.

Both microscopic structures may appear in DW superconductors. Nuclear magnetic resonance (NMR) experiments²⁰ are consistent with the scenario, where the phase separation takes place on the microscopic scale not exceeding the DW coherence length, thus supporting either of the above scenarios. In both scenarios, at low enough temperature, superconductivity appears at pressure $P > P_{c1}$,¹⁷ and the DW have a strong influence on the properties of such a mixed SC state. In particular, the SDW background suppresses the spin-singlet SC pairing, making spin-triplet pairing to be expected¹⁷ in agreement with experiments in $(\text{TMTSF})_2\text{PF}_6$.^{11,12,13} This feature appears due to the spin-dependent scattering on the SDW condensate, and it does not happen when superconductivity coexists with CDW.

In the present paper we follow the ideas of Ref. [17] and study in detail the microscopic structure and properties of the mixed SC-DW state in the first scenario of uniform DW with ungapped metallic pockets above $P > P_{c1}$. In Sec. II we generalize the model of Ref. [17] to the case of more realistic e-e interaction with backward and forward scattering, and describe in detail the uniform DW state with ungapped pockets. In Sec. III we estimate the SC transition temperature and the upper critical field H_{c2} in the DW-SC mixed state, and show, that H_{c2} strongly increases as pressure approaches the critical value P_{c1} , in agreement with experiments in $(\text{TMTSF})_2\text{PF}_6$ and α -(BEDT-TTF)₂KHg(SCN)₄. In Sec. IV we study SC on SDW background and show that SDW suppresses the spin-singlet SC ordering. Our results are aimed mainly to quasi-1D metals, but also can be applied to other DW superconductors with slightly imperfect nesting.

II. THE MODEL AND THE DW STATE WITHOUT SUPERCONDUCTIVITY

In quasi-1D metals the free electron dispersion without magnetic field writes down as

$$\varepsilon(\mathbf{k}) = \pm v_F(k_x \mp k_F) + t_{\perp}(\mathbf{k}_{\perp}). \quad (1)$$

The electron dispersion in the easy-conducting (chain) x -direction is strong and can be linearized near the Fermi surface (FS). The interchain dispersion $t_{\perp}(\mathbf{k}_{\perp})$ is much weaker and given by the tight-binding model with few

leading terms:

$$t_{\perp}(\mathbf{k}_{\perp}) = 2t_b \cos(k_y b) + 2t'_b \cos(2k_y b) + 2t_c \cos(k_z \tilde{c}), \quad (2)$$

where b, \tilde{c} are the lattice constants in the y - and z -direction. The dispersion along the z -axis is considerably weaker than along the y -direction and does not play any role in the analysis below. The FS consists of two warped sheets and possesses an approximate nesting property, $\varepsilon(\mathbf{k}) \approx -\varepsilon(\mathbf{k}-\mathbf{Q})$, which leads to the formation of DW at low temperature. The nesting property is only spoiled by the second term $t'_b(k_y)$ in Eq. (2), which, therefore, is called the "antinesting" term. Increase of the latter with applied pressure leads to the transition in the gapped DW state at $P = P_{c1}$, where the ungapped pockets on the FS or isolated soliton walls⁷ first appear. In the pressure interval $P_{c1} < P < P_c$ the new state develops, where the DW coexists with superconductivity at rather low temperature $T < T_c^{SC}$, while at high temperature $T > T_{SC}$ the DW state coexists with the normal metal phase.

The electron Hamiltonian is

$$\hat{H} = \hat{H}_0 + \hat{H}_{\text{int}}, \quad (3)$$

with the free-electron part in momentum representation

$$\hat{H}_0 = \sum_{\mathbf{k}} \varepsilon(\mathbf{k}) a_{\alpha}^{\dagger}(\mathbf{k}) a_{\alpha}(\mathbf{k}) \quad (4)$$

and the interaction part

$$\begin{aligned} \hat{H}_{\text{int}} = & \frac{1}{2} \sum_{\mathbf{k}, \mathbf{k}', \mathbf{Q}} V_{\alpha\beta\gamma\delta}(\mathbf{Q}) a_{\alpha}^{\dagger}(\mathbf{k} + \mathbf{Q}) a_{\beta}(\mathbf{k}) \\ & \times a_{\gamma}^{\dagger}(\mathbf{k}' - \mathbf{Q}) a_{\delta}(\mathbf{k}'). \end{aligned} \quad (5)$$

Here and below we imply the summation over repeating spin indices. The interaction potential is

$$V_{\alpha\beta\gamma\delta}(\mathbf{Q}) = U_c(\mathbf{Q}) - U_s(\mathbf{Q}) \vec{\sigma}_{\alpha\beta} \vec{\sigma}_{\gamma\delta}, \quad (6)$$

where $\vec{\sigma}_{\alpha\beta}$ are the Pauli matrices. For the formation of DW, the value of this potential at the nesting vector $\mathbf{Q} = \mathbf{Q}_N$ is only important. The values $U_c(\mathbf{Q}_N)$ and $U_s(\mathbf{Q}_N)$ are called the charge and spin coupling constants. Depending on their ratio, the charge or spin density wave is formed.

For superconducting pairing, both the momentum and frequency dependence of the potential (6) is important, being different for different compounds. Below we consider only a simplified model, similar to the BCS model,²¹ where the frequency dependence of the interaction potential is taken into account only through the ultraviolet cutoff (Debye frequency) in the Cooper loop. The phonon-mediated electron pairing produces only the spin-independent charge coupling $U_c(\mathbf{Q})$, and in the study of superconductivity we put $U_s(\mathbf{Q}) = 0$. As concerns the momentum dependence of $U_c(\mathbf{Q})$, in 1D

and quasi-1D metals one, usually, distinguishes only the backward and forward scattering:

$$U_c(\mathbf{Q}) = \begin{cases} U_c^f, & Q_x \ll 2k_F \\ U_c^b, & Q_x \approx 2k_F \end{cases}. \quad (7)$$

Depending on the signs and the ratio of backward U_c^b and forward U_c^f coupling constants, one has singlet or triplet SC pairing. The Hamiltonian (3) does not include the spin-orbit interaction, which is assumed to be weak.

Below we assume the DW transition temperature to be much greater than the SC transition temperature, $T_c^{DW} \gg T_c^{SC}$, which corresponds to most DW superconductors. For example, in (TMTSF)₂PF₆ $T_c^{SDW} \approx 8.5K \gg T_c^{SC} \approx 1.1K$, and in α -(BEDT-TTF)₂KHg(SCN)₄, $T_c^{CDW} \approx 8K \gg T_c^{SC} \approx 0.1K$. Therefore, we first study the structure of the DW state in the pressure interval $P_{c1} < P < P_c$, and then consider the superconductivity on this background.

A. The uniform DW state with ungapped states

In the case of the uniform DW order parameter, $\Delta_0(x) = \Delta_0 = \text{const}(T, P)$, the electron Green functions in the DW state in the mean-field approximation can be written down explicitly. We introduce the thermodynamic Green function

$$\hat{g}_{\alpha\beta}(\mathbf{k}', \mathbf{k}, \tau - \tau') = \langle T_\tau \{ a_\alpha^\dagger(\mathbf{k}', \tau') a_\beta(\mathbf{k}, \tau) \} \rangle, \quad (8)$$

where the operators are taken in the Heisenberg representation, and the Green function $\hat{g}_{\alpha\beta}(\mathbf{k}', \mathbf{k}, \tau - \tau')$ is an operator in the spin space. The CDW order parameter

$$\hat{\Delta}_{\mathbf{Q}} = U_c \sum_{\mathbf{k}} \hat{g}(\mathbf{k} - \mathbf{Q}, \mathbf{k}, -0) = \Delta_{\mathbf{Q}} \quad (9)$$

is a unity operator in spin space, and the SDW order parameter is

$$\hat{\Delta}_{\mathbf{Q}\alpha\beta} = U_s (\vec{\sigma}_{\alpha\beta} \cdot \vec{\sigma}_{\gamma\delta}) \sum_{\mathbf{k}} \hat{g}_{\gamma\delta}(\mathbf{k} - \mathbf{Q}, \mathbf{k}, -0) = (\vec{\sigma}\vec{l})\Delta_{\mathbf{Q}}, \quad (10)$$

where the complex vector \vec{l} determines the polarization of the SDW. In the presence of magnetic field \vec{H} and without internal magnetic anisotropy, $\vec{l} \perp \vec{H}$. Below the external magnetic field is taken to be rather weak to only affect SC but not the DW,²² because strong magnetic field would suppress SC. We consider only one DW order parameter, i.e. $\Delta_{\mathbf{Q}} \neq 0$ only for $\mathbf{Q} = \pm\mathbf{Q}_N$, where $\mathbf{Q}_N \approx 2k_F \mathbf{e}_x + (\pi/b)\mathbf{e}_y + (\pi/\tilde{c})\mathbf{e}_z$, and $\mathbf{e}_x, \mathbf{e}_y, \mathbf{e}_z$ are the unit vectors in x, y, z directions. In the mean-field approximation one has

$$\hat{H}_{\text{int}} = \frac{1}{2} \sum_{\mathbf{Q}\mathbf{k}} a_\alpha^\dagger(\mathbf{k} + \mathbf{Q}) a_\beta(\mathbf{k}) \hat{\Delta}_{\mathbf{Q}\alpha\beta}.$$

Hermicity of the Hamiltonian requires $\hat{\Delta}_{-\mathbf{Q}\alpha\beta} = \hat{\Delta}_{\mathbf{Q}\beta\alpha}^*$. Below we omit the explicit spin indices, keeping only the

“hat” symbol above the spin operators. For SDW the equations of motion in the frequency representation are

$$[i\omega - \varepsilon(\mathbf{k})]\hat{g}(\mathbf{k}', \mathbf{k}, \omega) - \sum_{\mathbf{Q}} \Delta_0(\vec{\sigma}\vec{l})\hat{g}(\mathbf{k}', \mathbf{k} - \mathbf{Q}, \omega) = \delta_{\mathbf{k}'\mathbf{k}} \quad (11)$$

If we neglect the scattering into the states with $|k_x| \gtrsim 2k_F$, the equations (11) decouple:

$$\begin{pmatrix} i\omega_n - \varepsilon(\mathbf{k}) & \Delta_0(\vec{\sigma}\vec{l}) \\ \Delta_0^*(\vec{\sigma}\vec{l}) & i\omega_n - \varepsilon(\mathbf{k} - \mathbf{Q}) \end{pmatrix} \hat{G} = \hat{I}, \quad (12)$$

where the matrix Green function

$$\hat{G} \equiv \begin{pmatrix} g^{RR}(\mathbf{k}, \mathbf{k}, \omega) & g^{LR}(\mathbf{k} - \mathbf{Q}, \mathbf{k}, \omega)(\vec{\sigma}\vec{l}) \\ g^{RL}(\mathbf{k}, \mathbf{k} - \mathbf{Q}, \omega)(\vec{\sigma}\vec{l}) & g^{LL}(\mathbf{k} - \mathbf{Q}, \mathbf{k} - \mathbf{Q}, \omega) \end{pmatrix}, \quad (13)$$

\hat{I} is the 2×2 identity matrix, and the R and L superscripts denote the right and left FS sheet of electrons:

$$a_\alpha(\mathbf{k}, \tau) \equiv \begin{cases} a_\alpha^R(\mathbf{k}, \tau), & k_x > 0 \\ a_\alpha^L(\mathbf{k}, \tau), & k_x < 0 \end{cases}. \quad (14)$$

The electron Green functions in the CDW state are obtained from Eqs. (12),(13) by removing the spin factor $(\vec{\sigma}\vec{l})$ from the nondiagonal elements.

Introducing the notations

$$\varepsilon_\pm(\mathbf{k}', \mathbf{k}) = [\varepsilon(\mathbf{k}') \pm \varepsilon(\mathbf{k})] / 2 \quad (15)$$

and

$$E_{1,2}(\mathbf{k}) \equiv \varepsilon_+(\mathbf{k}, \mathbf{k} - \mathbf{Q}) \pm \sqrt{\varepsilon_-^2(\mathbf{k}, \mathbf{k} - \mathbf{Q}) + |\Delta_0|^2}, \quad (16)$$

from (12) one has

$$g^{LR}(\mathbf{k} - \mathbf{Q}, \mathbf{k}, \omega) = \frac{\Delta_0}{[i\omega - E_1(\mathbf{k})][i\omega - E_2(\mathbf{k})]}, \quad (17)$$

$$g^{RL}(\mathbf{k}, \mathbf{k} - \mathbf{Q}, \omega) = \frac{\Delta_0^*}{[i\omega - E_1(\mathbf{k})][i\omega - E_2(\mathbf{k})]},$$

and

$$g^{RR}(\mathbf{k}, \mathbf{k}, \omega) = \frac{i\omega - \varepsilon(\mathbf{k})}{[i\omega - E_1(\mathbf{k})][i\omega - E_2(\mathbf{k})]} = g^{LL}(\mathbf{k}, \mathbf{k}, \omega). \quad (18)$$

The ungapped pockets on the Fermi surface with energy spectrum (16) appear when $|\varepsilon_+(\mathbf{k})|_{\text{max}} = 2t_b' > |\Delta_0|$, and these pockets are responsible for the Cooper instability at $P > P_{c1}$. With the tight-binding dispersion (2) at $P > P_{c1}$ there are four ungapped pockets on each of the two sheets of the original Fermi surface: two electron pockets with $E_2(k) = \varepsilon_+(\mathbf{k}) + \sqrt{\varepsilon_-^2(\mathbf{k}) + |\Delta_0|^2} < 0$ at $k_{y\text{max}}b = \pi/2, 3\pi/2$ and $k_{x\text{max}} = k_F$, and two hole pockets with $E_1(k) = \varepsilon_+(\mathbf{k}) - \sqrt{\varepsilon_-^2(\mathbf{k}) + |\Delta_0|^2} > 0$ at $k_{y\text{max}}b = 0, \pi$ and $k_{x\text{max}} = k_F \pm 2t_b/v_F$ (see Fig. 1). The

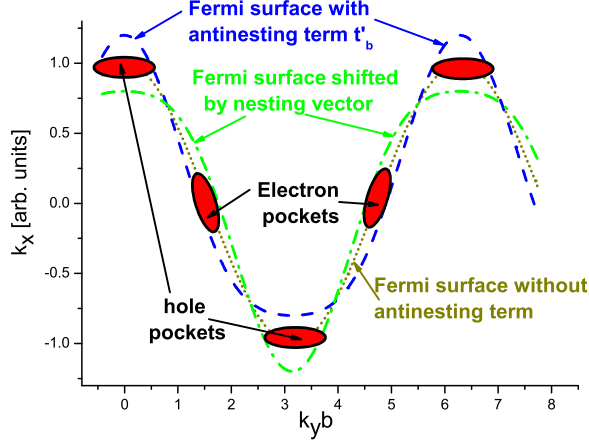


FIG. 1: (Color online) The schematic picture of small open pockets on one Fermi surface sheet, which get formed when the antinesting term ε_+ in Eq. (16) exceeds the DW energy gap Δ_0 . The blue dashed line shows the Fermi surface sheet with imperfect nesting, i.e. with $2t'_b > \Delta_0$. The green dash-dotted line shows the other Fermi surface sheet shifted by the nesting vector. If the nesting was perfect, these two lines would coincide. The dotted brown line shows the perfectly nested Fermi surface sheet. The red solid ellipses are the small Fermi surface pockets, that appear in the DW state when $2t'_b > \Delta_0$, i.e. when pressure exceeds P_{c1} .

hole pockets of the new FS are the elongated ellipses, satisfying $E_1(\mathbf{k}) = 0$ and having the main axes along the vectors \mathbf{k}_x and \mathbf{k}_y . Two electron pockets are the similar ellipses, rotated in the k_x - k_y plane by the angles

$$\phi_e = \pm \arctan(2t_b b / \hbar v_F). \quad (19)$$

Near the points $\mathbf{k} = \mathbf{k}_{\max}$, where $|\varepsilon_+(\mathbf{k})|$ has a maximum and the small ungapped pockets get formed, the dispersion (16) rewrites as $(\Delta k_y = k_y - k_{y\max})$

$$E_1(\Delta k_y, \varepsilon_-) \approx -\delta + a_1 (\Delta k_y)^2 + b_1 \varepsilon_-^2, \quad (20)$$

where using (2) one obtains

$$\varepsilon_-(\mathbf{k}) \approx v_F(k_x - k_F) - 2t_b b \sin(k_{y\max} b) \Delta \mathbf{k}_y / \hbar, \quad (21)$$

$$\begin{aligned} \delta &\equiv |\varepsilon_+(\mathbf{k})|_{\max} - |\Delta_0| = 2t'_b - |\Delta_0|, \\ a_1 &\approx 4t'_b{}^2 \text{ and } b_1 \approx 1/2\Delta_0. \end{aligned} \quad (22)$$

Here δ has the meaning of the Fermi energy in these small pockets,²⁸ and the last term in Eq. (21) rotates the electron FS pockets by the angle (19).

Without DW ordering, the density of states (DoS) of electrons with quasi-1D dispersion (1) is

$$\rho_0(E_F) = \int \frac{dk_x dk_y}{(2\pi)^2} \delta[\hbar v_F(k_x \pm k_F)] = \frac{1}{\pi \hbar v_F b}.$$

Let us estimate the DoS, on the Fermi level in the DW phase when the open pockets just appear. By definition²⁹

$$\rho(\varepsilon) = -(1/\pi) \text{Im}[\text{Tr}G_{ret}(\varepsilon)], \quad (23)$$

The retarded Green function is obtained from (18) by the analytical continuation $i\omega \rightarrow \varepsilon + i0$. Its substitution to (23) gives the DoS on the Fermi level (at $\varepsilon = 0$)

$$\rho(E_F) = \sum_{\mathbf{k}} \left(\frac{\varepsilon(\mathbf{k})}{E_1(\mathbf{k})} \delta[E_2(\mathbf{k})] + \frac{\varepsilon(\mathbf{k})}{E_2(\mathbf{k})} \delta[E_1(\mathbf{k})] \right), \quad (24)$$

where $\delta[x]$ is the Dirac δ -function. For small FS pockets, i.e. at $\delta \ll \Delta_0$, the residues of the Green function poles

$$\frac{\varepsilon(\mathbf{k})}{E_1(\mathbf{k})} = \frac{\varepsilon(\mathbf{k})}{E_2(\mathbf{k})} \approx \frac{1}{2},$$

and the contribution of one ungapped FS pocket per one spin orientation is given by

$$\begin{aligned} \rho_1 &= \int \frac{dk_x d\Delta k_y}{(2\pi)^2} \frac{\delta[a_1(\Delta k_y)^2 + b_1 \varepsilon_-^2 - \delta]}{2} \\ &= \int \frac{dxdy/(2\pi)^2}{\hbar v_F \sqrt{a_1 b_1}} \frac{\delta(x^2 + y^2 - \delta)}{2} \\ &= \int \frac{dr^2/8\pi}{\hbar v_F b} \delta(r^2 - \delta) = \frac{1}{8\pi \hbar v_F b}. \end{aligned}$$

There are 8 ungapped pockets for the dispersion (2), and the total DoS on the Fermi level per one spin component in DW state is the same as without DW ordering:

$$\rho(E_F) = 8\rho_1 = \frac{1}{\pi \hbar v_F b}. \quad (25)$$

This result differs from that in the previously studied models^{5,6}, where the electron spectrum on the ungapped parts of the FS does not change after the formation of DW, and the DoS on the Fermi level reduces when the DW is formed, so that the SC transition temperature reduces exponentially. In our model, the DoS on the Fermi level in the DW state with open FS pockets is the same as without DW. Therefore, the SC transition temperature in our model does not change so strong when the DW ordering with ungapped pockets is destroyed completely with the restoration of the metallic state (see Sec. III A for more details). The DoS on the Fermi level also determines many other physical properties.

B. Stability with respect to superconductivity in the metallic state

The phonon-mediated electron pairing produces only the charge coupling $U_c(\mathbf{Q})$, and in the study of superconductivity, one may use the hamiltonian (5)-(7), neglecting the coupling $U_s(\mathbf{Q})$ in (6). Then, in terms of

left and right moving electrons, the interaction Hamiltonian has the form

$$\begin{aligned} \hat{H}_{\text{int}} = & \frac{1}{2} \sum_{\mathbf{k}\mathbf{k}'\mathbf{Q}} U_c^b a_\alpha^{\dagger R}(\mathbf{k} + \mathbf{Q}) a_\alpha^L(\mathbf{k}) a_\beta^{\dagger L}(\mathbf{k}' - \mathbf{Q}) a_\beta^R(\mathbf{k}') \\ & + \frac{1}{2} \sum_{\mathbf{k}\mathbf{k}'\mathbf{Q}} U_c^f a_\alpha^{\dagger R}(\mathbf{k} + \mathbf{Q}) a_\alpha^R(\mathbf{k}) a_\beta^{\dagger L}(\mathbf{k}' - \mathbf{Q}) a_\beta^L(\mathbf{k}'). \end{aligned} \quad (26)$$

With two FS sheets in (1), it is useful to describe SC in terms of two Gor'kov functions²⁹

$$F^{L(R)R(L)}(X_1, X_2) = \langle T(\hat{\Psi}^{L(R)}(X_1)\hat{\Psi}^{R(L)}(X_2)) \rangle, \quad (27)$$

where $X = (\tau, \mathbf{r})$, and $\hat{\Psi}^{L(R)}(X)$ are the field operators for the left and right parts of the Brillouin zone, formally, comprising the electrons with momenta $P_{\parallel} < 0$ (L) and $P_{\parallel} > 0$ (R). The averages in (27) at $\tau_1 = \tau_2 + 0$

$$\begin{aligned} \hat{f}_{\alpha\beta}^{LR}(\mathbf{r}) &= \langle \hat{\Psi}_\alpha^L(\mathbf{r})\hat{\Psi}_\beta^R(\mathbf{r}) \rangle; \\ \hat{f}_{\alpha\beta}^{RL}(\mathbf{r}) &= \langle \hat{\Psi}_\alpha^R(\mathbf{r})\hat{\Psi}_\beta^L(\mathbf{r}) \rangle \end{aligned} \quad (28)$$

have the meaning of the Cooper pair wave function and determine the SC order parameter $\hat{\Delta}_{SC}(\mathbf{r})$. The "hat" above the functions $\hat{f}^{LR}(\mathbf{r})$ and $\hat{\Delta}_{SC}(\mathbf{r})$ means that these functions are operators in the spin space. In the materials with spatial inversion symmetry, like (TMTSF)₂PF₆, one has $\hat{f}^{LR} = \pm \hat{f}^{RL}$, and the sign (\pm) depends on whether the SC pairing is singlet (+) or triplet (-). Below we assume the uniform SC order parameter: $\hat{f}_{\alpha\beta}^{LR}(\mathbf{r}) = \hat{f}_{\alpha\beta}^{LR}$. In the momentum representation Eq. (28) rewrites

$$\begin{aligned} \hat{f}_{\alpha\beta}^{LR} &= \sum_{\mathbf{k}} \langle a_\alpha^L(\mathbf{k}) a_\beta^R(-\mathbf{k}) \rangle; \\ \hat{f}_{\alpha\beta}^{RL} &= \sum_{\mathbf{k}} \langle a_\alpha^R(\mathbf{k}) a_\beta^L(-\mathbf{k}) \rangle. \end{aligned} \quad (29)$$

We introduce the notation for the Cooper bubble:

$$\Pi_d = T \sum_{\mathbf{k}, \omega} g^{RR}(\mathbf{k}, \mathbf{k}, \omega) g^{LL}(-\mathbf{k}, -\mathbf{k}, -\omega), \quad (30)$$

where the Green functions $g^{RR(LL)}(\mathbf{k}, \mathbf{k}, \omega)$ in the metallic state given by Eq. (18) at $\Delta_0 = 0$. From the Hamiltonian (26) with definition (30) one obtains the Gor'kov equations for the onset of SC:

$$\begin{aligned} \hat{f}^{LR} &= - \left(U_c^b \hat{f}^{RL} + U_c^f \hat{f}^{LR} \right) \Pi_d, \\ \hat{f}^{RL} &= - \left(U_c^b \hat{f}^{LR} + U_c^f \hat{f}^{RL} \right) \Pi_d. \end{aligned} \quad (31)$$

Eq. (31) is shown schematically in Fig. 2. Summation and subtraction of the two lines in Eq. (31) gives the equations on SC transition temperature T_{c0}^{SC} in the metallic state:

$$\begin{aligned} \hat{f}^{LR} + \hat{f}^{RL} &= - (U_c^f + U_c^b) \left(\hat{f}^{LR} + \hat{f}^{RL} \right) \Pi_d, \\ \hat{f}^{LR} - \hat{f}^{RL} &= - (U_c^f - U_c^b) \left(\hat{f}^{LR} - \hat{f}^{RL} \right) \Pi_d. \end{aligned} \quad (32)$$

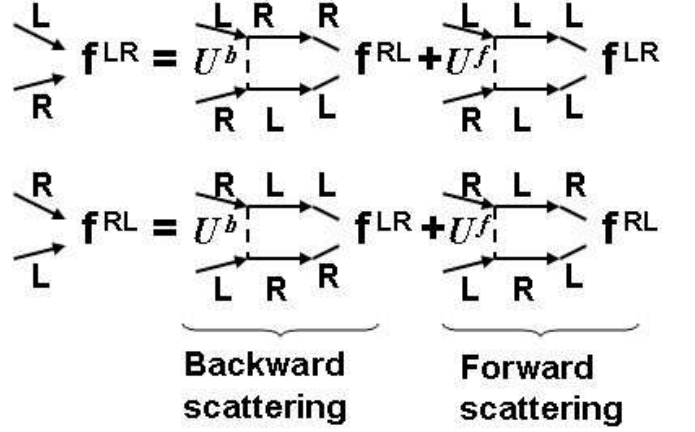


FIG. 2: The diagram equations for the Gor'kov functions \hat{f}^{LR} and \hat{f}^{RL} without DW. The solid lines represent the electron Green functions: $g^{RR(LL)}(\mathbf{k}, \omega)$ in the metallic state. The dashed lines represent the short-range e-e interaction U_c^f or U_c^b .

The first line in Eq. (32) corresponds to singlet, and the second line to the triplet pairing. Usually, $-U_c^f - U_c^b > U_c^b - U_c^f$, and the singlet SC transition temperature is higher. Eq. (32) rewrites as

$$1 = g\Pi_d, \quad g = \max \{ -U_c^f - U_c^b, U_c^b - U_c^f \}. \quad (33)$$

Therefore, in our model one has singlet or triplet superconductivity depending on the ratio of the coupling constants U_c^f and U_c^b . The nonmagnetic impurities also suppress the triplet SC ordering. The Cooper bubble Π_d has the well-known logarithmic singularity, appearing after the summation over momenta and frequencies:

$$\Pi_d^{met} = \Pi_d^{met}(T) \approx \nu_F \ln(\bar{\omega}/T), \quad (34)$$

where $\bar{\omega}$ is a proper cutoff,²⁹ and $\nu_F = \rho_0(E_F)$ is the density of states at the Fermi level. For the quasi-1D electron spectrum (1), $\nu_F = 1/\pi\hbar v_F b$. From (33),(34) one obtains the equation for the SC critical temperature T_{c0}^{SC} :

$$1 \approx g\nu_F \ln(\bar{\omega}/T_{c0}^{SC}). \quad (35)$$

III. SC IN THE CDW STATE

First, we study the SC instability in the CDW state, where the spin structures of the CDW and SC order parameters do not interfere. As we shall see below in Sec. IV, the results obtained in this section for the spin-singlet superconductivity on the CDW background can be applied with little modification for the triplet superconductivity on the SDW background. The problem of SC instability and the upper critical field H_{c2} on the CDW background is important itself. The organic metal α -(BEDT-TTF)₂KHg(SCN)₄ gives an example, where the

interplay of superconductivity and CDW leads to the new SC properties,⁹ and there are many other CDW superconductors.¹

The basic equations for the CDW state without superconductivity are obtained from Eqs. (13)-(22) by removing the spin factor ($\vec{\sigma}\vec{l}$) from the nondiagonal elements in Eqs. (11)-(13). Thus, the matrix Green function in the uniform CDW state without SC resembles Eq. (13):

$$\hat{G} \equiv \begin{pmatrix} g^{RR}(\mathbf{k}, \mathbf{k}, \omega) & g^{LR}(\mathbf{k} - \mathbf{Q}, \mathbf{k}, \omega) \\ g^{RL}(\mathbf{k}, \mathbf{k} - \mathbf{Q}, \omega) & g^{LL}(\mathbf{k} - \mathbf{Q}, \mathbf{k} - \mathbf{Q}, \omega) \end{pmatrix}, \quad (36)$$

with the matrix components given by Eqs. (17)-(18). In addition to the term (30), the Cooper bubble on the DW background contains another term, coming from the nondiagonal elements in the Green function (36):

$$\Pi_n = T \sum_{\mathbf{k}, \omega} g^{LR}(\mathbf{k} - \mathbf{Q}, \mathbf{k}, \omega) g^{RL}(-\mathbf{k} + \mathbf{Q}, -\mathbf{k}, -\omega). \quad (37)$$

Therefore, the Gor'kov equations on the DW background acquire two additional terms as compared to Eq. (31):

$$\begin{aligned} \hat{f}^{LR} &= - \left(U_c^b \hat{f}^{RL} + U_c^f \hat{f}^{LR} \right) \Pi_d - \left(U_c^b \hat{f}^{LR} + U_c^f \hat{f}^{RL} \right) \Pi_n, \\ \hat{f}^{RL} &= - \left(U_c^b \hat{f}^{LR} + U_c^f \hat{f}^{RL} \right) \Pi_d - \left(U_c^b \hat{f}^{RL} + U_c^f \hat{f}^{LR} \right) \Pi_n. \end{aligned} \quad (38)$$

In writing these equations we use that the spin structure of the Gor'kov functions \hat{f}^{LR} commutes with the Green functions $g^{R(L)R(L)}(\mathbf{k}, \mathbf{k}', \omega)$ on the CDW background. Eq. (38) is shown schematically in Fig. 3.

The summation and subtraction of the two lines in Eq. (38) give the equation on the SC transition temperature for singlet and triplet pairing respectively:

$$\begin{aligned} \hat{f}^{LR} + \hat{f}^{RL} &= - (U_c^f + U_c^b) \left(\hat{f}^{LR} + \hat{f}^{RL} \right) (\Pi_d + \Pi_n), \\ \hat{f}^{LR} - \hat{f}^{RL} &= - (U_c^f - U_c^b) \left(\hat{f}^{LR} - \hat{f}^{RL} \right) (\Pi_d - \Pi_n). \end{aligned} \quad (39)$$

Below we show that Π_d and Π_n have the same sign, and $|\Pi_d + \Pi_n| > |\Pi_d - \Pi_n|$. Therefore, if in the metallic state the transition temperature to singlet SC T_{cSC}^{Singlet} is higher than T_{cSC}^{Triplet} to the triplet SC, then on the CDW background $T_{cSC}^{\text{Singlet}} > T_{cSC}^{\text{Triplet}}$ is also valid. For SDW, the interplay of the spin structures of SC and SDW produces important changes (see Sec. IV).

A. SC instability and transition temperature in the uniform CDW state

The equation on the singlet SC transition temperature T_{cCDW}^{SC} on CDW background, given by the first line in Eq. (39), writes down as $K_1 \equiv g(\Pi_d + \Pi_n) = 1$, where

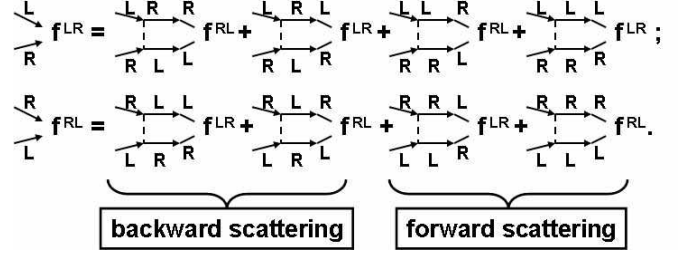


FIG. 3: The diagram equations for the Gor'kov functions \hat{f}^{LR} and \hat{f}^{RL} in the presence of the DW ordering with two coupling constants. The solid lines represent the electron Green functions $g_n^{R(L)R(L)}(k, \omega)$ in the DW state. The dashed lines represent the short-range e-e interaction, i.e. backward g_b or forward g_f scattering.

for singlet pairing $g = -(U_c^f + U_c^b)$. Using $\varepsilon(\mathbf{k}) = \varepsilon(-\mathbf{k})$ and substituting (17),(18), we obtain

$$K_1 = Tg \sum_{\mathbf{k}, \omega_n} \frac{\omega^2 + [\varepsilon_-(\mathbf{k}) + \varepsilon_+(\mathbf{k})]^2 + |\Delta_0|^2}{[\omega^2 + E_1^2(\mathbf{k})][\omega^2 + E_2^2(\mathbf{k})]} \quad (40)$$

$$= \frac{Tg}{2} \sum_{\mathbf{k}, \omega_n} \left(\frac{1}{\omega^2 + E_1^2(\mathbf{k})} + \frac{1}{\omega^2 + E_2^2(\mathbf{k})} \right) \quad (41)$$

$$= \frac{g}{v_F} \int_0^{2\pi/b} \frac{bdk_y}{2\pi} \int_{-\bar{\omega}}^{\bar{\omega}} \frac{d\varepsilon_- \tanh[E_1(\mathbf{k})/2T]}{E_1(\mathbf{k})} \quad (42)$$

In writing the second line, Eq. (41), we have substituted (16) and used the symmetry of the functions $\varepsilon_{\pm}(k_y)$: $\varepsilon_+(k_y)$ is an even function of k_y , and $\int dk_y F(\varepsilon_{\pm}(k_y)) = 0$ for any odd function $F(\varepsilon)$. Let us now rewrite $K_1 \equiv K_{ult} + K_{inf}$, where

$$\begin{aligned} K_{ult} &\equiv \frac{g}{v_F} \int_0^{2\pi/b} \frac{bdk_y}{2\pi} \int_{|\Delta_0|}^{\bar{\omega}} \frac{d\varepsilon_- \tanh[E_1(\mathbf{k})/2T]}{\pi E_1(\mathbf{k})} \\ &\approx [g/\pi v_F] \ln(\bar{\omega}/\Delta_0) \end{aligned} \quad (43)$$

contains the ultraviolet logarithmic divergence in expression (42), and

$$K_{inf} \equiv \frac{g}{v_F} \int_0^{2\pi/b} \frac{bdk_y}{2\pi} \int_0^{|\Delta_0|} \frac{d\varepsilon_- \tanh[E_1(\mathbf{k})/2T]}{\pi E_1(\mathbf{k})} \quad (44)$$

may contain the infrared logarithmic divergence if there are electron states on the Fermi level. At $P > P_{c1}$ the ungapped electron states appear as small Fermi-surface pockets (see Sec. IIA and Fig. 1), or as the soliton band.¹⁷ In each case, the formed small "Fermi surface" is subjected to the Cooper instability at rather low temperature, which signifies the possibility for the onset of SC pairing.

Substituting (20) for $E_1(\mathbf{k})$ in Eq. (44) and introducing $r^2 \equiv a_1(\Delta k_y)^2 + b_1\varepsilon^2$, we obtain

$$\begin{aligned} K_{inf} &\approx \frac{N_P^e g b / v_F}{4\pi \sqrt{a_1 b_1}} \int_0^{\Delta_0} \frac{\tanh[(\delta - r^2)/2T]}{\delta - r^2} dr^2 \\ &\approx \frac{N_P^e g}{2\pi v_F \sqrt{2t_b'/\Delta_0}} \ln \left[C \sqrt{\Delta_0 \delta} / T \right], \end{aligned} \quad (45)$$

where $C \sim 1$ is a numerical constant, and N_P^e is the number of ungapped electron pockets on one FS sheet. With the tight-binding dispersion (2), at $2t'_b > \Delta_0$ in each Brillouin zone $N_P^e = 2$ (see Fig. 1). Thus, when the small pockets just appear, i.e. when $0 < 2t'_b/\Delta_0 - 1 \ll 1$,

$$K_1 \approx \frac{g}{\pi v_F} \left[\ln(\bar{\omega}/\Delta_0) + \ln\left(C\sqrt{\Delta_0\delta}/T\right) \right]. \quad (46)$$

Comparing Eqs. (46) and (35) one obtains, that the SC critical temperature T_{cCDW}^{SC} in the CDW state is related to the SC transition temperature T_{c0}^{SC} without CDW as

$$T_{cCDW}^{SC} \approx CT_{c0}^{SC} \sqrt{\delta/\Delta_0}. \quad (47)$$

This result differs from Eqs. 3.5 and 3.7 of Ref.⁶, where T_{cCDW}^{SC} was exponentially smaller than T_{c0}^{SC} . The origin of this difference was explained in the end of Sec. IIB, where the DoS on the Fermi level in the DW state with small open pockets and in the metallic state were shown to be approximately the same. The assumption that the electron spectrum in the ungapped FS pockets does not change after the formation of DW, used in Refs. [5,6], is not valid, especially when the ungapped FS pockets are small. For quasi-1D tight-binding dispersion (1)-(2), the SC transition temperature on the CDW background with ungapped FS pockets T_{cCDW}^{SC} is only slightly less than T_{c0}^{SC} .

Eqs. (43)-(47) were derived following Ref. [17] with logarithmic accuracy, i.e. assuming $\ln(\delta/T) \gg 1$ and $\ln(\Delta_0/\delta) \gg 1$. This accuracy is not sufficient to determine the constant C . For more accurate estimate of the transition temperature T_{cCDW}^{SC} , we calculated the integral (42) numerically for the particular dispersion (2). This calculation confirms the approximate formula (47) at $\delta \ll \Delta_0$, and gives the value of the constant $C \approx 1.86$ (see Fig. 4). At $\delta/t'_b \ll 1$ the analytical and numerical results coincide, while at $\delta \sim t'_b$ the ratio $T_{cCDW}^{SC}(\delta)/T_{c0}^{SC}$ tends to saturate, being always less than unity. In agreement with Eq. (47), the ratio $T_{cCDW}^{SC}/T_{c0}^{SC}$ is almost independent of T_{c0}^{SC} .

The above analytical and numerical estimations show, that the CDW state with ungapped pockets on the Fermi surface is always unstable toward the formation of the superconductivity, and the SC transition temperature T_{cCDW}^{SC} on the CDW background is not very low, being slightly less than the SC transition temperature T_{c0}^{SC} without CDW. The formation of the ungapped pockets in the CDW state due to the increase of the antinesting term at $P > P_{c1}$ is, usually, accompanied by the reduction of the CDW energy gap Δ_0 and, hence, by the fast growth of the size $\delta(P)$ of the ungapped FS pockets. Then, from Eq. (47) we obtain, that the SC critical temperature T_{cCDW}^{SC} (47) also grows very rapidly at $P > P_{c1}$. In experiment, this fast growth of $T_{cCDW}^{SC}(P)$ above P_{c1} may be similar to the jump of T_{cCDW}^{SC} from zero to some finite value.

The fluctuations and change of the phonon modes, accompanying the transition from CDW to metallic state

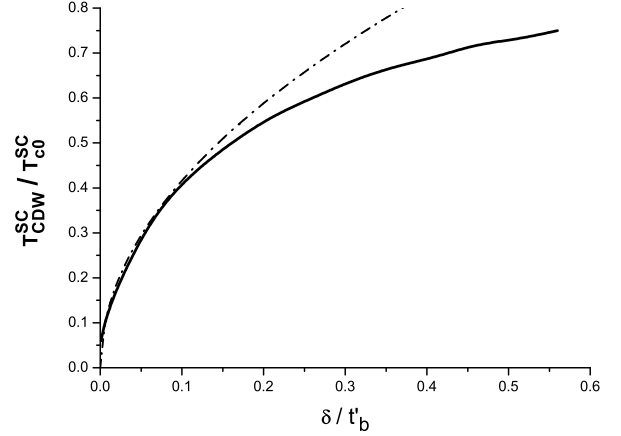


FIG. 4: The SC transition temperature T_{cCDW}^{SC} on the CDW background in the pocket scenario. The solid line shows the ratio $T_{cCDW}^{SC}/T_{c0}^{SC}$, calculated numerically from Eq. (42), as function of the size δ of the ungapped Fermi surface pockets. The dash-dotted line represents the analytical formula (47) with the numerically calculated constant $C \approx 1.86$.

in the whole pressure interval $P_{c1} \lesssim P \lesssim P_{c1}$, may considerably increase the SC transition temperature T_{cCDW}^{SC} and influence the dependence $T_{cCDW}^{SC}(P)$. CDW also affects the screening of the Coulomb interaction, which changes the e-e coupling and the SC transition temperature. Even a small change in the e-e coupling constant leads to the dramatic changes in the SC transition temperature.²⁹ An accurate calculation of $T_{cCDW}^{SC}(P)$ on the DW background must take these two effects into account, being beyond the scope of the present paper.

B. Upper critical field H_{c2} in the SC state on the uniform CDW background

Upper critical field in superconductors with intrinsic DW ordering was considered theoretically in the model,³⁰ where the DW gap appears only on those FS sections, where the nesting condition is fulfilled, while on the rest of FS the electron spectrum has no singularities. This is not the case for our model (see Sec. II), where the dispersion of the ungapped electrons in DW state have singularity at $P \rightarrow P_{c1}$, which affect the SC properties and H_{c2} . Other calculations^{31,32} of H_{c2} in DW superconductors also use the models very different from the one considered in Sec. II.

To calculate the upper critical field H_{c2} , let us use the Ginzburg-Landau (G-L) approximation. The main contribution to the gradient term comes from the ungapped pockets of the Fermi surface ($|\varepsilon_+(\mathbf{k})| > \Delta_0$). For arbitrary electron dispersion, the G-L functional was derived in Ref. [34]. The order parameter in the general form is

a function of two wave vectors:

$$\Delta(\mathbf{k}_1, \mathbf{k}_2) = \Delta_{\mathbf{q}}(\mathbf{k}) = \Delta(\mathbf{q}) \psi(\mathbf{k}),$$

where the vector $\mathbf{q} = \mathbf{k}_1 + \mathbf{k}_2$ gives the spatial modulation of the SC order parameter $\Delta(\mathbf{r}) = \int d\mathbf{q} \Delta(\mathbf{q}) e^{i\mathbf{q}\mathbf{r}}$, and $\mathbf{k} = \mathbf{k}_1$ is the momentum of an electron in a Cooper pair. In the case of s-pairing, $\psi(\mathbf{k}) = \text{const} = 1$. For triplet-pairing $\Delta_{\mathbf{q}}(\mathbf{k}) = -\Delta_{\mathbf{q}}(-\mathbf{k})$, and for the quasi-1D dispersion (2) with two separated FS sheets we may take $\psi(\mathbf{k}) = \text{sign}(k_x)$. To calculate the gradient term in the Ginzburg-Landau expansion, we use Eq. (11) of Ref. [34], which gives the G-L equation for the order parameter in the form

$$\sum_{j,k} \frac{1}{2m_{jk}} [\nabla_j + 2ieA_j(\mathbf{r})] [\nabla_k + 2ieA_k(\mathbf{r})] \Delta(\mathbf{r}) + T \left\{ \frac{T_c^{SC} - T}{T_c^{SC}} - f |\Delta(\mathbf{r})|^2 \Delta(\mathbf{r}) \right\} = 0, \quad (48)$$

where $A_j(\mathbf{r})$ is the vector potential,

$$\frac{1}{m_{jk}} = \frac{7\xi(3)}{12\pi^2 T} \int \mathbf{v}_j \mathbf{v}_k \psi^2(\mathbf{k}) \frac{d\sigma_F}{|\mathbf{v}|} / \int \frac{d\sigma_F}{|\mathbf{v}|} \quad (49)$$

$$\equiv \frac{7\xi(3)}{12\pi^2 T} \frac{\int \mathbf{v}_j \mathbf{v}_k \psi^2(\mathbf{k}) d^3\mathbf{k} \delta(E(\mathbf{k}) - E_F)}{\int \psi^2(\mathbf{k}) d^3\mathbf{k} \delta(E(\mathbf{k}) - E_F)},$$

$$f = \frac{7\xi(3)}{8(\pi T)^2} \int \psi^4(\mathbf{k}) \frac{d\sigma_F}{|v_F^*|}, \quad (50)$$

and $\int d\sigma_F$ is the integral over the Fermi surface in the momentum space. Since the G-L equation (48) was derived at $T_c^{SC} - T \ll T_c^{SC}$, one can replace T by T_c^{SC} in Eqs. (49),(50). Introducing the notations

$$k_x^* = k_x - k_F; \quad k_y^* \equiv \Delta k_y \left(2b\sqrt{2t'_b \Delta_0 / \hbar v_F} \right),$$

one rewrites the dispersion (20) for the hole pockets of the FS as

$$E(\mathbf{k}^*) = \frac{(\hbar v_F)^2}{2\Delta_0} [k_y^{*2} + k_x^{*2}] - \delta. \quad (51)$$

The Fermi surface, $E(\mathbf{k}^*) = 0$, is parameterized by the angle ϕ , where $\tan \phi \equiv k_y^*/k_x^*$. The quasi-particle velocity on the FS is a function of this angle:

$$v_x = v_F \sqrt{2\delta/\Delta_0} \cos \phi;$$

$$v_y = (4b/\hbar) \sqrt{\delta t'_b} \sin \phi.$$

Performing the integrations in (49), we obtain the contribution from each hole pocket to the tensor (49):

$$\left(\frac{1}{m_{xx}} \right)_h = \frac{7\xi(3)}{12\pi^2 T_c^{SC}} \frac{v_F^2}{\Delta_0} \left(\frac{\delta}{\Delta_0} \right); \quad (52)$$

$$\left(\frac{1}{m_{yy}} \right)_h = \frac{14\xi(3) b^2 t'_b \delta}{3\pi^2 \hbar^2 T_c^{SC}}; \quad \left(\frac{1}{m_{xy}} \right)_h = 0.$$

This mass tensor is very anisotropic:

$$\left(\frac{m_{yy}}{m_{xx}} \right)_h = \frac{\hbar^2 v_F^2}{8t'_b \Delta_0 b^2} \sim \left(\frac{\hbar v_F}{2bt'_b} \right)^2 \gg 1.$$

The contribution from the electron pockets can be obtained via the rotation of tensor (52) by the angles (19):

$$\left(\frac{1}{m_{xx}} \right)_e = \left(\frac{1}{m_{xx}} \right)_h \cos^2 \phi_e + \left(\frac{1}{m_{yy}} \right)_h \sin^2 \phi_e$$

$$\left(\frac{1}{m_{yy}} \right)_e = \left(\frac{1}{m_{xx}} \right)_h \sin^2 \phi_e + \left(\frac{1}{m_{yy}} \right)_h \cos^2 \phi_e.$$

The nondiagonal elements $(1/m_{xy})_e$ vanish after the summation over two electron pockets, which are rotated in the opposite directions. The total G-L mass tensor is

$$\frac{1}{m_{ij}} = 4 \left[\left(\frac{1}{m_{ij}} \right)_e + \left(\frac{1}{m_{ij}} \right)_h \right],$$

and, using $|\phi_e| = \arctan(2t_b b / \hbar v_F) \ll 1$, we obtain

$$\frac{1}{m_{xx}} \approx \frac{14\xi(3) v_F^2}{3\pi^2 T_c^{SC}} \left(\frac{\delta}{\Delta_0} \right); \quad (53)$$

$$\frac{1}{m_{yy}} \approx \frac{7\xi(3) v_F^2}{3\pi^2 T_c^{SC}} \left(\frac{\delta}{\Delta_0} \right) \left(\frac{2t_b b}{\hbar v_F} \right)^2.$$

From the Ginzburg-Landau equation one obtains the i -component of the upper critical field

$$H_{c2}^i = e_{ijk} \frac{(T_c^{SC} - T) c}{e\hbar} \sqrt{m_j m_k}, \quad (54)$$

where e_{ijk} is the antisymmetric tensor of rang 3. For $H \parallel z$, the substitution of (53) in (54) gives

$$H_{c2}^z = C_1 \cdot \left(\frac{T_c^{SC}}{\delta} \right) \frac{c (T_c^{SC} - T)}{b v_F e}, \quad (55)$$

where

$$C_1 = \frac{3\pi^2}{7\xi(3) \sqrt{2}} \left(\frac{\Delta_0}{2t_b} \right). \quad (56)$$

The estimate of the constant (56) is very sensitive to the electron dispersion (2), e.g., to the presence of the fourth harmonic $2t_4 \cos(4k_y b)$ in Eq. (2). The fourth harmonic with $t_4/t_2 > 0$ increases the size δ of the ungapped hole pockets at $k_y b \approx \pi n$ by $2t_4$, reducing by the same amount the size of the electron pockets at $k_y b \approx \pi(n + 1/2)$. If $2t_4 > \delta$, the electron pockets disappear, and only the hole pockets contribute to the mass tensor (49). The total mass tensor is then very anisotropic and given by Eq. (52) multiplied by the number of the hole pockets. Its substitution to Eq. (54) gives (we take $\Delta_0/2t'_b \approx 1$)

$$C_1 = 3\pi^2/14\xi(3) = 1.76, \quad (57)$$

which is greater than (56) by a factor $\sim t_b/t'_b$. The similar increase of the constant C_1 also appears if the

DW wave vector \mathbf{Q} shifts from $\mathbf{Q}_0 = (2k_F, \pi/b)$, so that the electron pockets disappear, while the size δ of the hole pockets increases. Accurate calculation of the constant C_1 requires the detailed knowledge of electron dispersion.

According to Eq. (55), H_{c2}^z diverges as $P - P_{c1} \rightarrow 0$. If $\delta \propto P - P_{c1}$,²⁸ assuming $T_c^{SC} \approx \text{const}$, one obtains $H_{c2}^z \propto 1/(P - P_{c1})$. In our model, according to (47), $T_c^{SC} \propto \sqrt{\delta} \propto \sqrt{P - P_{c1}}$, and from (55) one obtains the square-root divergence of H_{c2}^z :

$$H_{c2}^z(P) \approx H_{c0}/\sqrt{P/P_{c1} - 1}. \quad (58)$$

The divergence of H_{c2}^z as pressure approaches P_{c1} has been observed in the mixed state in (TMTSF)₂PF₆ (see Fig. 2 in Ref. [14]) and also in α -(BEDT-TTF)₂KHg(SCN)₄ (see Figs. 5 and 6 of Ref. [9]). To explain this dependence $H_{c2}^z(P - P_{c1})$ in the scenario of the macroscopic spatial phase separation,¹⁴ the width d_S of the superconducting domains must be taken much smaller than the SC coherence length ξ_{SC} , because in a thin type-II-superconductor slab of thickness $d_s \ll \xi_{SC}$ the upper critical field H_{c2} is higher than in the bulk superconductor by a factor (see Eq. 12.4 of Ref. [35])

$$H_{c2}/H_{c2}^0 \approx \sqrt{12}\xi_{SC}/d_s. \quad (59)$$

In the discussion of Ref. [14] the penetration length λ instead of the coherence length ξ_{SC} enters the expression for H_{c2} in a thin superconducting slab, which is correct only for type I superconductors. If $d_s \ll \xi_{SC}$, the domain size d_s is of the order of the DW coherence length, which may cost additional energy because of the change of the DW structure. Then, the soliton scenario¹⁷ of the DW/SC structure is possible.

The available experimental data in (TMTSF)₂PF₆ is not sufficient to determine the behavior of $T_c^{SC}(P)$ close to the critical pressure $P = P_{c1}$, which is important for

quantitative comparison of the dependence $H_{c2}(P)$ in Eqs. (55),(58) with experiment. We only make the order-of-magnitude comparison with experiment to check if the model is reasonable. In (TMTSF)₂PF₆ the Fermi velocity $v_F \approx 2 \cdot 10^7$ cm/sec, the interchain spacing $b \approx 7.7\text{\AA}$, and $\Delta_0/2t_b \approx t'_b/t_b \approx 0.1$. Substituting this and $\delta \approx T_c^{SC}$ into Eq. (55) gives the slope $dH_{c2}^z/dT \approx 1$ Tesla/ $^\circ K$ in a reasonable agreement with the experimental data at $P \rightarrow P_{c1}$ (see Fig. 2 in Ref. [14]).

In α -(BEDT-TTF)₂KHg(SCN)₄ the Fermi velocity³⁶ $v_F \approx 6.5 \cdot 10^6$, the lattice constant³⁷ $b \approx 10\text{\AA}$, the SC and CDW transition temperatures⁹ $T_c^{SC} \approx 0.1K$ and $T_c^{CDW} \approx 8K$. Although the original Fermi surface in this compound possesses the quasi-2D pockets in addition to the quasi-1D sheets subjected to the CDW instability, the quasi-1D FS sheets seem to play an important role in the formation of SC, because superconductivity appears in the presence of CDW (at $P < P_c$) with approximately the same transition temperature T_c^{SC} as in the absence of CDW at $P > P_c$. Hence, SC and CDW share the same quasi-1D conducting band. In this compound $P_c \approx 2.5$ kbar,⁹ while P_{c1} and $\delta(P)$ are not known. Probably, even at ambient pressure $P > P_{c1}$ and $\delta \lesssim \Delta_0$. Substitution of $\delta \approx \Delta_0/2$ to Eq. (55) gives the estimate $dH_{c2}^z/dT \approx (1 - T/T_c^{SC}) \cdot 3.2mT$ in agreement with experiment (see Figs. 5 of Ref. [9]).

IV. SUPERCONDUCTING INSTABILITY IN THE SDW STATE

The Green functions in the SDW state are given by Eqs. (13)-(18), and the Gor'kov equations for SC in the SDW state, shown schematically in Fig. 3, write down as

$$\begin{aligned} \hat{f}^{LR} = & -TU_c^b \sum_{\mathbf{k}, \omega} \left[g^{RR}(\mathbf{k}, \mathbf{k}, \omega) \hat{f}^{RL} g^{LL}(-\mathbf{k}, -\mathbf{k}, -\omega)^T + g^{LR}(\mathbf{k} - \mathbf{Q}, \mathbf{k}, \omega) (\vec{\sigma}\vec{l}) \hat{f}^{LR} (\vec{\sigma}\vec{l})^T g^{RL}(\mathbf{Q} - \mathbf{k}, -\mathbf{k}, -\omega) \right] \\ & - TU_c^f \sum_{\mathbf{k}, \omega} \left[g^{LL}(-\mathbf{k}, -\mathbf{k}, -\omega) \hat{f}^{LR} g^{RR}(\mathbf{k}, \mathbf{k}, \omega)^T + g^{RL}(-\mathbf{k} + \mathbf{Q}, -\mathbf{k}, -\omega) (\vec{\sigma}\vec{l}) \hat{f}^{RL} (\vec{\sigma}\vec{l})^T g^{LR}(\mathbf{k} - \mathbf{Q}, \mathbf{k}, \omega) \right] \end{aligned} \quad (60)$$

and

$$\begin{aligned} \hat{f}^{RL} = & -TU_c^b \sum_{\mathbf{k}, \omega} \left[g^{LL}(-\mathbf{k}, -\mathbf{k}, -\omega) \hat{f}^{LR} g^{RR}(\mathbf{k}, \mathbf{k}, \omega)^T + g^{RL}(\mathbf{Q} - \mathbf{k}, -\mathbf{k}, -\omega) (\vec{\sigma}\vec{l}) \hat{f}^{RL} (\vec{\sigma}\vec{l})^T g^{LR}(\mathbf{k} - \mathbf{Q}, \mathbf{k}, \omega) \right] \\ & - TU_c^f \sum_{\mathbf{k}, \omega} \left[g^{RR}(\mathbf{k}, \mathbf{k}, \omega) \hat{f}^{RL} g^{LL}(-\mathbf{k}, -\mathbf{k}, -\omega)^T + g^{LR}(\mathbf{k} - \mathbf{Q}, \mathbf{k}, \omega) (\vec{\sigma}\vec{l}) \hat{f}^{LR} (\vec{\sigma}\vec{l})^T g^{RL}(\mathbf{Q} - \mathbf{k}, -\mathbf{k}, -\omega) \right]. \end{aligned} \quad (61)$$

The spin structure of the Gor'kov functions \hat{f}^{LR} , which depend on the type of SC pairing, interferes with the spin structure $(\vec{\sigma}\vec{l})$ of the SDW order parameter. This considerably changes the properties of SC on the SDW background as compared those on CDW background, studied in Sec. III.

With notations (30) and (37), Eqs. (60) and (61) rewrite as

$$\hat{f}^{LR} + \hat{f}^{RL} = -T (U_c^b + U_c^f) \left[\Pi_d (\hat{f}^{RL} + \hat{f}^{LR}) + \Pi_n (\vec{\sigma}\vec{l}) (\hat{f}^{LR} + \hat{f}^{RL}) (\vec{\sigma}\vec{l})^T \right] \quad (62)$$

$$\hat{f}^{LR} - \hat{f}^{RL} = -T (U_c^b - U_c^f) \left[\Pi_d (\hat{f}^{RL} - \hat{f}^{LR}) + \Pi_n (\vec{\sigma}\vec{l}) (\hat{f}^{LR} - \hat{f}^{RL}) (\vec{\sigma}\vec{l})^T \right]. \quad (63)$$

A. SC transition temperature

1. Singlet pairing.

For spin-singlet pairing $\hat{f}^{LR} = \hat{f}^{RL} = \hat{\sigma}_y f^{LR}$. Since

$$\hat{\sigma}_y (\vec{\sigma}\vec{l})^T = -(\vec{\sigma}\vec{l}) \hat{\sigma}_y, \quad (64)$$

Eq. (62) becomes

$$f^{LR} + f^{RL} = - (U_c^b + U_c^f) (f^{LR} + f^{RL}) (\Pi_d - \Pi_n). \quad (65)$$

Substituting Eqs. (30),(37) to (62) and using $\varepsilon(\mathbf{k}) = \varepsilon(-\mathbf{k})$ we rewrite equation (65) as $K_{SDW}^s = 1$, where

$$K_{SDW}^s = Tg \sum_{\mathbf{k}, \omega_n} \frac{\omega^2 + [\varepsilon_-(\mathbf{k}) + \varepsilon_+(\mathbf{k})]^2 - |\Delta_0|^2}{[\omega^2 + E_1^2(\mathbf{k})][\omega^2 + E_2^2(\mathbf{k})]} = 1. \quad (66)$$

This formula differs from the similar equation (40) for CDW by the sign before $|\Delta_0|^2$ in the numerator. This sign change, coming from the interplay (64) of the spin structures of SDW and SC order parameters, is crucial for the SC transition temperature. As in the case of CDW, the ungapped pockets of the FS appear when $|\varepsilon_+(\mathbf{k})|_{\max} > |\Delta_0|$, and these pockets are responsible for the low-energy logarithmic singularity of K_1 at $T \rightarrow 0$. If the system is close to the phase transition at $P = P_{c1}$, where these pockets just appear, the antineesting term in the electron dispersion only slightly exceeds the SDW gap, and $|\varepsilon_+(\mathbf{k})|_{\max} - |\Delta_0| = \delta \ll |\Delta_0|$. Then in these ungapped pockets $|\varepsilon_-(\mathbf{k})| \sim \delta \ll |\Delta_0|$, and the numerator in (66) near $\omega \rightarrow 0$ has the smallness $\delta/|\Delta_0| \ll 1$ as compared to the case of CDW. This leads to the same smallness of the logarithmically singular term in K_{SDW}^s at $T \rightarrow 0$. Instead of the Eq. (42) one now obtains

$$K_{SDW}^s \approx \frac{g}{2} \sum_{\mathbf{k}} \frac{\tanh [E_1(\mathbf{k})/2T]}{E_1(\mathbf{k})} \left(1 - \frac{4|\Delta_0|^2}{E_2^2(\mathbf{k})} \right). \quad (67)$$

When the ungapped pockets are small, the extra factor $[1 - 4|\Delta_0|^2/E_2^2(\mathbf{k})] \sim \delta/\Delta_0 \ll 1$ makes the infrared divergent term in expression (67) much smaller than in Eq. (42) for the CDW background. Therefore, the spin-singlet SC transition temperature on the SDW background is exponentially smaller as compared to Eq. (47):

$$T_{cSDW}^{SC} \sim \sqrt{\Delta_0 \delta} (T_{c0}^{SC}/\Delta_0)^{(\Delta_0/\delta)}. \quad (68)$$

The estimates (47),(68) depend strongly on the electron dispersion.

2. Triplet pairing.

The smallness $\sim \delta/\Delta_0$ of the numerator in Eq. (66) always appears for spin-singlet SC pairing on the SDW background. However, it does not necessarily appear for spin-triplet pairing. The triplet order parameter has the spin structure $\hat{f}^{LR} = \hat{\sigma}_y (\hat{\sigma}\vec{\mathbf{d}}) f^{LR}$. Substituting it together with $f^{RL} = -f^{LR}$ into (63), using $(\vec{\sigma}\vec{l}) (\hat{\sigma}\vec{\mathbf{d}}) = -(\hat{\sigma}\vec{\mathbf{d}}) (\vec{\sigma}\vec{l}) + 2(\vec{\mathbf{d}}\vec{l})$ and

$$(\vec{\sigma}\vec{l}) (\hat{\sigma}\vec{\mathbf{d}}) \hat{\sigma}_y (\vec{\sigma}\vec{l})^T = (\hat{\sigma}\vec{\mathbf{d}}) \hat{\sigma}_y - 2(\vec{\mathbf{d}}\vec{l}) (\vec{\sigma}\vec{l}) \hat{\sigma}_y, \quad (69)$$

we obtain the self-consistency equation

$$(f^{LR} - f^{RL}) (\hat{\sigma}\vec{\mathbf{d}}) = (U_c^b - U_c^f) (f^{LR} - f^{RL}) \times \left((\hat{\sigma}\vec{\mathbf{d}}) \Pi_d - [(\hat{\sigma}\vec{\mathbf{d}}) - 2(\vec{\mathbf{d}}\vec{l}) (\vec{\sigma}\vec{l})] \Pi_n \right). \quad (70)$$

For $\vec{\mathbf{d}} \parallel \vec{l}$ the equation on SC transition temperature is the same as in the case of singlet SC on the CDW background [see the first line of Eq. (39)] with only the change of the coupling constant from $U_c^b + U_c^f$ to $U_c^b - U_c^f$. Hence, at $U_c^f \ll U_c^b$, the SC transition temperature T_c^{SC} for $\vec{\mathbf{d}} \parallel \vec{l}$ is approximately given by Eq. (47). For $\vec{\mathbf{d}} \perp \vec{l}$ one obtains the smallness $\sim \delta/\Delta_0$ of the infrared-divergent term in the Cooper bubble, as in the case of spin-singlet SC on the SDW background. Then the SC transition temperature T_c^{SC} is roughly given by Eq. (68), being exponentially smaller than in the case $\vec{\mathbf{d}} \parallel \vec{l}$. For other mutual orientation of vectors $\vec{\mathbf{d}}$ and \vec{l} , the spin structures of left and right parts of Eq. (70) do not coincide, which means the possible mixing of singlet and triplet states.

B. Upper critical field

As we have shown above, the spin-singlet superconductivity, appearing on the SDW background, has vanishing critical temperature. Hence, we consider only the triplet superconductivity at $\vec{\mathbf{d}} \parallel \vec{l}$, which corresponds to the highest critical temperature. For the triplet superconductivity, the paramagnetic spin effect of magnetic field due to the interaction with electron spin does not lead to the suppression of superconductivity, and the upper critical field H_{c2} is completely determined by the orbital electron motion. In the scenario of ungapped pockets, the upper

critical field H_{c2} on SDW background at $\tilde{\mathbf{d}} \parallel \vec{l}$ is approximately the same as for SC on the CDW background and is given by Eq. (55).

V. SUMMARY

We investigated the structure and the properties of superconductivity, appearing on the uniform DW background and sharing with DW the common conducting band. The onset of superconductivity requires ungapped electron states on the Fermi level, which appear at pressure $P > P_{c1}$, i.e. when the nesting of the FS is spoiled. There are two possible microscopic structures of the background DW state with such ungapped states on the Fermi level: (a) the DW energy gap does not cover the whole Fermi surface, i.e. there are ungapped FS pockets, and (b) the DW order parameter is not spatially uniform, and the soliton band get formed.¹⁷ In this paper the first scenario is considered in detail. The approach of Ref.¹⁷ is generalized to the more realistic e-e interaction, which includes two coupling constants. It is shown, that the electron dispersion in the ungapped FS pockets on the DW background is strongly different from that in the metallic state, so that even very small ungapped FS pockets create rather high DoS on the Fermi level. This fact makes our results very dissimilar to many previous theoretical approaches, where the electron dispersion on the un-nested parts of FS in DW state was taken the same as in the metallic state.^{5,6,7,30,31,33} For the tight-binding dispersion (1),(2) the DoS on the Fermi level in the DW state with small ungapped FS pockets is the same as in the metallic state without DW [see Eq. (25)]. Therefore, the SC transition temperature T_{cDW}^{SC} on the DW back-

ground with such ungapped FS pockets (i.e., at pressure $P > P_{c1}$) is not exponentially smaller than the SC transition temperature T_{c0}^{SC} in the metallic state [see Eq. (47)], and the quantum critical fluctuations at $P \approx P_{c1}$ may increase T_{cDW}^{SC} to the value even higher than T_{c0}^{SC} .

The DW background considerably changes the SC properties. The upper critical field H_{c2} has unusual pressure dependence [see Eq. (58)] and may considerably exceed H_{c2} without DW background. According to Eqs. (55) and (58), H_{c2} even diverges as $P \rightarrow P_{c1}$; this divergence is cut off at $\delta \sim T_c^{SC}$. The SDW background strongly suppresses the spin-singlet superconductivity, while the triplet SC with certain spin polarization ($\tilde{\mathbf{d}} \parallel \vec{l}$) on the SDW background behaves similarly to the singlet SC on the CDW background. This means that the SDW background spares the formation of triplet superconductivity compared to the spin-singlet SC. If both types of SC are possible, the system with SDW background will choose the triplet SC, even if it would choose singlet SC without SDW background. The results obtained are in good agreement with experimental observations in two organic metals (TMTSF)₂PF₆ and α -(BEDT-TTF)₂KHg(SCN)₄, where SC coexists with SDW and CDW states respectively, giving an alternative to Ref. [14] explanation of the unusual pressure dependence of H_{c2} in (TMTSF)₂PF₆ and some other compounds.

VI. ACKNOWLEDGEMENT

The work was supported by RFBR No 06-02-16551 and 06-02-16223, and by MK-4105.2007.2.

* Electronic address: grigorev@itp.ac.ru

† Visiting address: Institut Laue Langevin, Grenoble, France

¹ A.M. Gabovich, A.I. Voitenko, J.F. Annett and M. Ausloos, Supercond. Sci. Technol. **14**, R1-R27 (2001).

² K. Levin, D. L. Mills, and S. L. Cunningham, Phys. Rev. B **10**, 3821 (1974).

³ C. A. Balseiro and L. M. Falicov, Phys. Rev. B **20**, 4457 (1979).

⁴ L. Milans del Bosch and Felix Yndurain, Phys. Rev. B **41**, 2540 (1990).

⁵ Griff Bilbro and W. L. McMillan, Phys. Rev. B **14**, 1887 (1976).

⁶ K. Machida, J. Phys. Soc. Jpn. **50**, 2195 (1981).

⁷ G. C Psaltakis, J. Phys. C: Solid State Phys. **17**, 2145 (1984).

⁸ T. Vuletic, P. Auban-Senzier, C. Pasquier et al., Eur. Phys. J. B **25**, 319 (2002).

⁹ D. Andres, M. V. Kartsovnik, W. Biberacher, K. Neumaier, E. Schuberth, and H. Müller, Phys. Rev. B **72**, 174513 (2005).

¹⁰ A. M. Clogston, Phys. Rev. Lett. **9**, 266 (1962); B.S. Chan-

drasekhar, Appl. Phys. Lett. **1**, 7 (1962).

¹¹ I. J. Lee, M. J. Naughton, G. M. Danner, and P. M. Chaikin, Phys. Rev. Lett. **78**, 3555 (1997); I. J. Lee, P. M. Chaikin, and M. J. Naughton, Phys. Rev. B **62**, R14 669 (2000);

¹² I. J. Lee, P. M. Chaikin, and M. J. Naughton, Phys. Rev. B **65**, 180502(R) (2002).

¹³ I. J. Lee, S. E. Brown, W. G. Clark, M. J. Strouse, M. J. Naughton, W. Kang, and P. M. Chaikin, Phys. Rev. Lett. **88**, 017004 (2001); I.J. Lee, D. S. Chow, W. G. Clark, M. J. Strouse, M. J. Naughton, P. M. Chaikin, and S. E. Brown, Phys. Rev. B **68**, 092510 (2003).

¹⁴ I. J. Lee, P. M. Chaikin, and M. J. Naughton, Phys. Rev. Lett. **88**, 207002 (2002).

¹⁵ I. J. Lee, S. E. Brown, W. Yu, M. J. Naughton, and P. M. Chaikin, Phys. Rev. Lett. **94**, 197001 (2005).

¹⁶ L.P. Gor'kov, P.D. Grigorev, Europhys. Lett. **71**, 425 (2005).

¹⁷ L.P. Gor'kov, P.D. Grigoriev, Phys. Rev. B **75**, 020507(R) (2007).

¹⁸ S.A. Brazovskii and N.N. Kirova, Sov. Sci. Rev. A Phys., **5**, 99 (1984).

- ¹⁹ W.P. Su and J. R. Schrieffer, *Physics in One Dimension/* Ed. by J. Bernasconi and T. Schneider, Springer series in Solid State Sciences, Berlin, Heidelberg and New York: Springer, 1981.
- ²⁰ Stuart Brown, unpublished.
- ²¹ J. Bardeen, L. N. Cooper, and J. R. Schrieffer, *Phys. Rev.* **108**, 1175 (1957).
- ²² The generalization of the mean-field description of DW in quasi-1D metals in the presence of magnetic field was elaborated in Ref.²³ for SDW and in Refs. [24,25] for CDW. Strong magnetic field, acting on CDW state, mixes the SDW and CDW order parameters^{24,25} and may lead to the series of phase transitions between the states with different quantized values of the nesting vector.²⁶ Strong magnetic field, acting on metals with imperfect nesting, can lead to the field-induced DW.²⁷
- ²³ A. Bjeliš and D. Zanchi, *Phys. Rev. B* **49**, 5968 (1994).
- ²⁴ D. Zanchi, A. Bjeliš, and G. Montambaux, *Phys. Rev. B* **53**, 1240 (1996).
- ²⁵ P.D. Grigoriev and D.S. Lyubshin, *Phys. Rev. B* **72**, 195106 (2005).
- ²⁶ D. Andres, M. V. Kartsovnik, P. D. Grigoriev, W. Biberacher, and H. Müller, *Phys. Rev. B* **68**, 201101(R) (2003).
- ²⁷ L.P. Gor'kov and A.G. Lebed, *J. Phys. (Paris)* **45**, L433 (1984); G. Montambaux, M. Heritier, and P. Lederer, *Phys. Rev. Lett.* **55**, 2078 (1985); A.G. Lebed, *Phys. Rev. Lett.* **88**, 177001 (2002); A.G. Lebed, *JETP Lett.* **72**, 141 (2000) [*Pis'ma Zh. Teor. Eksp. Fiz.* **72**, 205 (2000)].
- ²⁸ Usually, $\delta \propto P - P_{c1}$. However, the reduction of the energy gap Δ_0 , accompanying the formation of ungapped pockets and the reduction of the nested part of FS, can make the growth $\delta(P)$ faster at $P = P_{c1}$.
- ²⁹ A.A. Abrikosov, L.P. Gor'kov and I.E. Dzyaloshinskii, "Methods of quantum field theory in statistical physics", Dover Publications, INC., New York 1977.
- ³⁰ A. M. Gabovich and A. S. Shpigel, *Phys. Rev. B* **38**, 297 (1988).
- ³¹ Charles Ro and K. Levin, *Phys. Rev. B* **29**, 6155 (1984).
- ³² Proposed in Ref. [33] appearance of an additional spatially modulated SC order parameter $\Delta_{SC}(Q_N)$ seems to be negligible (or wrong) when the Fermi energy is much greater than the DW and SC order parameters.
- ³³ Kazushige Machida, Tamotsu Kōnyama, and Takeo Matsubara, *Phys. Rev. B* **23**, 99 (1981).
- ³⁴ L.P. Gor'kov and T.K. Melik-Barkhudarov, *JETP* **18**, 1031 (1963) [*J. Exp. Teor. Fiz.* **45**, 1493 (1963)].
- ³⁵ J. B. Ketterson and S. N. Song, *Superconductivity*, Cambridge University Press, 1999.
- ³⁶ A. E. Kovalev, S. Hill, and J. S. Qualls, *Phys. Rev. B* **66**, 134513 (2002).
- ³⁷ Ryusuke Kondo, Seiichi Kagoshima and Mitsuhiro Maesato, *Phys. Rev. B* **67**, 134519 (2003).